

THE PHYSICAL REVIEW

A journal of experimental and theoretical physics established by E. L. Nichols in 1893

SECOND SERIES, VOL. 140, No. 1B

11 OCTOBER 1965

Gamma Rates and Intensities; l -Forbidden $M1$ Transitions

D. B. FOSSAN, L. F. CHASE, JR., AND K. L. COOP

Research Laboratories, Lockheed Missiles & Space Company, Palo Alto, California

(Received 24 May 1965)

A search for l -forbidden $M1$ transitions of the type ($1g_{7/2} \rightleftharpoons 2d_{5/2}$) has been made in Pm^{149} , Pm^{151} , and Sb^{125} . Lifetimes of the first excited states were obtained from beta-gamma and gamma-gamma time-delay distributions that were measured with a fast time-to-height converter. The measured half-life for the 114-keV level in Pm^{149} is (2.62 ± 0.10) nsec and that for the 326-keV level in Sb^{125} is ≤ 0.2 nsec; hindrance factors relative to Moszkowski limits for these transitions are 350 and ≤ 300 , respectively. In the deformed nucleus Pm^{151} , the half-life of the 118-keV first excited state is ≤ 0.3 nsec and that of the 256-keV level was measured to be (0.91 ± 0.03) nsec. Lifetime limits for additional levels were obtained. Because of uncertainties in the level schemes of Pm^{149} and Pm^{151} , the gamma-ray intensities from the decay of Nd^{149} and Nd^{151} were measured with a Ge(Li) solid-state detector. From the 28-h Pm^{151} daughter activity, a half-life of (0.48 ± 0.03) nsec was measured which is associated with the 105-keV level in Sm^{151} and an upper limit of ≤ 0.2 nsec was placed on the half-life of the 345-keV level.

I. INTRODUCTION

ODD-PROTON $M1$ transitions of the type ($1g_{7/2} \rightleftharpoons 2d_{5/2}$) are retarded from the theoretical Moszkowski estimate by factors of 100 to 1000.¹ These transitions that involve $\Delta J = \pm 1$, no change in parity, and $\Delta l = \pm 2$ are l -forbidden for the ordinary additive magnetic-dipole operator that requires $\Delta l = 0$. To account for the speeds of these l -forbidden transitions, two approaches have been used. The first allows the $M1$ transition to proceed by admixtures of different configurations in the initial- and final-state wave functions of the radiating particle,² while the second changes the form of the magnetic-dipole operator either by charge and spin exchange between nucleons³ or by spin-orbit coupling.⁴ More recently, it has been shown that collective quadrupole vibrations are in many cases sufficiently important, even for nuclei outside the deformed regions, to explain the $M1$ rates.⁵ Partial success has been obtained by these theories; however, none as yet predicts all the experimental information.

¹ *Nuclear Data Sheets*, compiled by K. Way *et al.* (Printing and Publishing Office, National Academy of Sciences-National Research Council, Washington 25, D. C.) NRC 5-5-vi.

² A. Arima, H. Horie, and M. Sano, *Progr. Theoret. Phys. (Kyoto)* **17**, 567 (1957).

³ R. G. Sachs and M. Ross, *Phys. Rev.* **84**, 379 (1961).

⁴ H. de Waard and T. R. Gerholm, *Nucl. Phys.* **1**, 281 (1956).

⁵ R. A. Sorensen, *Phys. Rev.* **132**, 2270 (1963).

A survey of hindrance factors for l -forbidden $M1$ transitions in odd-proton nuclei as a function of neutron number indicates a greater degree of forbiddenness in the vicinity of the closed shell of 82 neutrons.⁶ Further experimental information on such transitions in this region is of importance to establish these hindrance trends with more certainty. In this experiment, a search for odd-proton l -forbidden $M1$ transitions has been made for transitions from the first excited states in Pm^{149} , Pm^{151} , and Sb^{125} .

For Pm^{149} and Sb^{125} , the transitions between the first excited state and the ground state are of the type ($1g_{7/2} \rightleftharpoons 2d_{5/2}$); for Pm^{151} only the ground state is known to have a spin of $\frac{5}{2}$. In the case of Sb^{125} which has 74 neutrons, the $M1$ transition is made by an odd proton outside the closed shell of 50. The speeds of similar $M1$ transitions in three other antimony isotopes have previously been measured.⁷

Upon increasing the neutron number from 88 to 90, a rapid change in the nuclear structure takes place as a result of the shift from spherical to deformed equilibrium shapes. It is expected that the increased col-

⁶ H. de Waard (private communication); I. M. Goviland and C. S. Khurana, *Nucl. Phys.* **60**, 666 (1964).

⁷ T. D. Nainan, *Phys. Rev.* **123**, 1751 (1961); Y. Y. Chu, O. C. Kistner, A. C. Li, S. Monaro, and M. L. Perlman, *Phys. Rev.* **133**, B1361 (1964); M. Schmorak, A. C. Li, and A. Schwarzschild, *Phys. Rev.* **130**, 727 (1963).

lective effects that cause the deformation would reduce the amount of $M1$ l forbiddenness. This influence of collective motion on $(1g_{7/2} \rightarrow 2d_{5/2})$ $M1$ transitions has been observed for $\text{Eu}^{147,149,151}$ where the neutron number changes from 84 to 88.⁸ Another particularly suitable group of odd-proton nuclei for the study of these effects is $\text{Pm}^{145,147,149,151}$ where the neutron number changes from 84, a spherical nucleus, to 90, a deformed nucleus. The rates of $(1g_{7/2} \leftrightarrow 2d_{5/2})$ $M1$ transitions have previously been measured for Pm^{145} and Pm^{147} .⁹ It is hoped that the collective influence on such $M1$ transitions can be further understood from information obtained for the other two promethium isotopes Pm^{149} and Pm^{151} .

Initial lifetime measurements¹⁰ on the first excited state of Pm^{149} were based on the Nd^{149} decay scheme of Rutledge *et al.*¹¹ where the only betas above 1.1 MeV in energy were those associated with the 1.5-MeV beta transition to this state at 114 keV. In this lifetime measurement, betas with energies above 1.1 MeV were used as a time indication for the formation of this state; the measured lifetime was consistent with an l -forbidden $M1$ transition. After these measurements were made, a publication of the decay studies for Nd^{149} by Gopinathan and Joshi¹² showed that the previously thought of 1.5-MeV beta transition consisted of several beta branches. In order to eliminate the possibility of interfering lifetimes that could result from the other branches, the lifetime of the 114-keV state was re-measured with higher bias conditions in order to isolate the betas populating this state. Because of a measurable lifetime for a level at higher energy in Pm^{149} , which was populated by one of these beta branches, the new result was 8% less. More recently, level scheme studies for the Nd^{149} decay have been published by Currie *et al.*¹³ and Chen *et al.*¹⁴ A number of uncertainties exist regarding level energies and gamma-ray transitions. For interpretation of the present lifetime work, and to better establish the gamma-ray transitions between levels in Pm^{149} , the gamma rays following the decay of Nd^{149} were studied with a Ge(Li) solid-state detector.¹⁵ The improved energy resolution for this gamma-ray detector is a great advantage over that obtainable from NaI crystals which were employed in the previous work. Currie *et al.*¹³ also measured several lifetimes of levels in Pm^{149} ; these results

are in general agreement with the present experiment. Also, to interpret an observed lifetime for a low-energy level in Pm^{151} , the gamma-ray spectrum from 12-min Nd^{151} was measured with the Ge(Li) detector. Only very limited information was available on the decay scheme of Pm^{151} .

After the completion of the investigation of 12-min Nd^{151} , the daughter activity of 28-h Pm^{151} was used to study lifetimes of levels in Sm^{151} .

II. EXPERIMENT

The lifetime measurements in the present experiment were made with a time-to-height converter using a fast-slow coincidence technique in a manner similar to that described previously.¹⁶ Activities for the measurements, 1.8-h Nd^{149} , 12-min Nd^{151} , and 9.7-min Sm^{125} , were produced from separated isotopes by neutron capture in the Stanford University reactor. The separated isotopes were obtained in oxide form from Oak Ridge National Laboratory. Because of the short-lived activities, the measurements were made by observing time-delay distributions between betas and gammas rather than between betas and conversion electrons. With the method used, no additional time is wasted in making thin sources. Groups of measurements were made as a function of counting rate while the sources decayed to allow discrimination against any counting-rate effects. The betas and gammas which mark the population and decay of the nuclear states were detected with 1-in.-diam by 1-in.-long NE102 plastic scintillators coupled to 7264A RCA phototubes. One measurement was made with gamma-gamma coincidences. A Cronetics fast time-to-height converter was used along with a

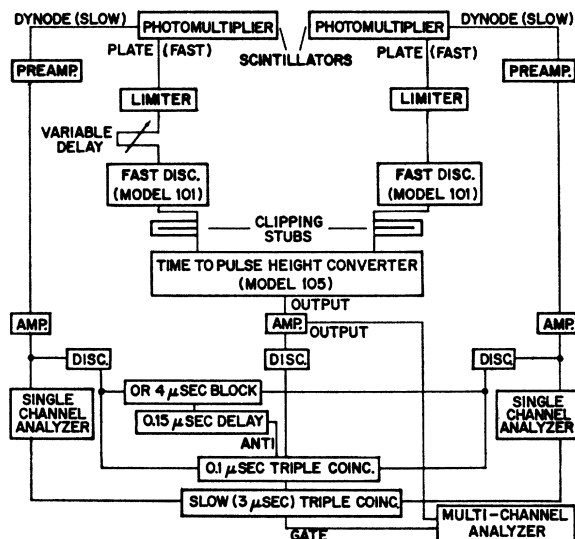


FIG. 1. A schematic diagram of the lifetime-measurement apparatus.

⁸ E. Ye. Berlovich, Yu. K. Gusev, V. V. Ilyin, V. V. Nikitin, and M. K. Nikitin, *Nucl. Phys.* **37**, 469 (1962).

⁹ R. L. Graham and R. E. Bell, *Can. J. Phys.* **31**, 377 (1953); E. Ye. Berlovich, G. M. Bukat, Yu. K. Gusev, V. V. Ilyin, V. V. Nikitini, and M. K. Nikitin, *Phys. Letters* **2**, 344 (1962).

¹⁰ D. B. Fossan, *Bull. Am. Phys. Soc.* **9**, 663 (1964).

¹¹ W. C. Rutledge, J. M. Cork, and S. B. Burson, *Phys. Rev.* **86**, 775 (1952).

¹² K. P. Gopinathan and M. C. Joshi, *Phys. Rev.* **134**, B297 (1964).

¹³ W. M. Currie and P. W. Dougan, *Nucl. Phys.* **61**, 561 (1965).

¹⁴ C. H. Chen and R. G. Arns, *Nucl. Phys.* **63**, 233 (1965).

¹⁵ A. J. Tavendale and G. T. Ewan, *Nucl. Instr. Methods* **25**, 185 (1963).

¹⁶ D. B. Fossan and B. Herskind, *Nucl. Phys.* **40**, 24 (1963).

multicoincidence circuit for the slow-pulse coincidence requirements. The slow-pulse channel widths were kept at approximately 25% of the maximum accepted pulse height. A 4- μ sec blocking circuit¹⁷ for the elimination of pile-up effects was employed because of the relatively high singles rates used. A schematic diagram of the experimental apparatus is shown in Fig. 1.

The performance of the system is shown in Fig. 2 by the two resolution functions obtained with prompt Co⁶⁰ gammas. The curve with open circles was obtained with both acceptance channels at about 1 MeV; the width at half-maximum is 380 psec and the left slope corresponds to a half-life of 65 psec. The resolution curve with filled circles (insert) was obtained with one of the channels placed at a 30-keV Compton-electron energy which corresponds to about 100-keV gamma rays; for this case the width at half-maximum is about 1 nsec while the left slope corresponds to a half-life of 200 psec. Time calibration of the time-to-height converter was made with air-dielectric lines.

Pm¹⁴⁹

The lifetime of the $\frac{5}{2}^+$ level in Pm¹⁴⁹ at 114 keV decaying to the $\frac{7}{2}^+$ ground state was measured using the 1.8-h beta activity of Nd¹⁴⁹. The gamma-ray spectrum following the beta decay of Nd¹⁴⁹ was measured with a 5-mm thick Ge(Li) solid-state detector. The observed gamma-ray spectrum is shown in Fig. 3; in these measurements the betas were stopped with the appropriate thickness of Al. From energy and efficiency calibrations with known sources, the gamma-ray ener-

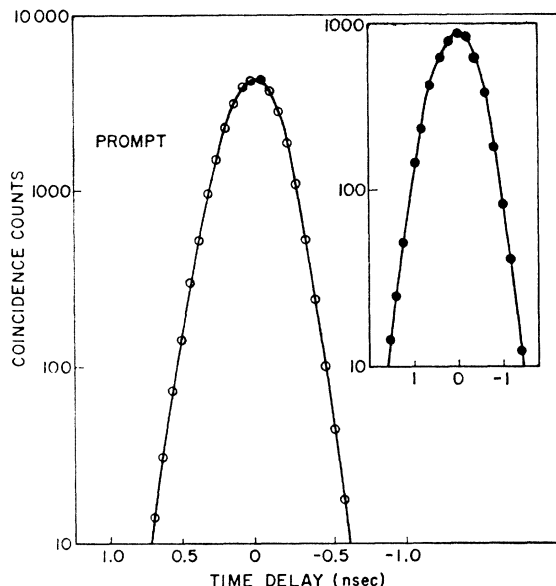


FIG. 2. Prompt-resolution function from Co⁶⁰ with narrow channels at about 1 MeV. The prompt-resolution function taken with one of the channels at 30 keV is shown in the insert with filled circles.

gies and intensities have been obtained; the results are listed in Table I. A decay scheme of Nd¹⁴⁹ is shown in Fig. 4; the levels of Pm¹⁴⁹ are from previous work¹¹⁻¹⁴; however, the precise energies shown are obtained from the present gamma-ray measurements. A number of observed gamma rays do not fit this level scheme; no attempt has been made to include them.

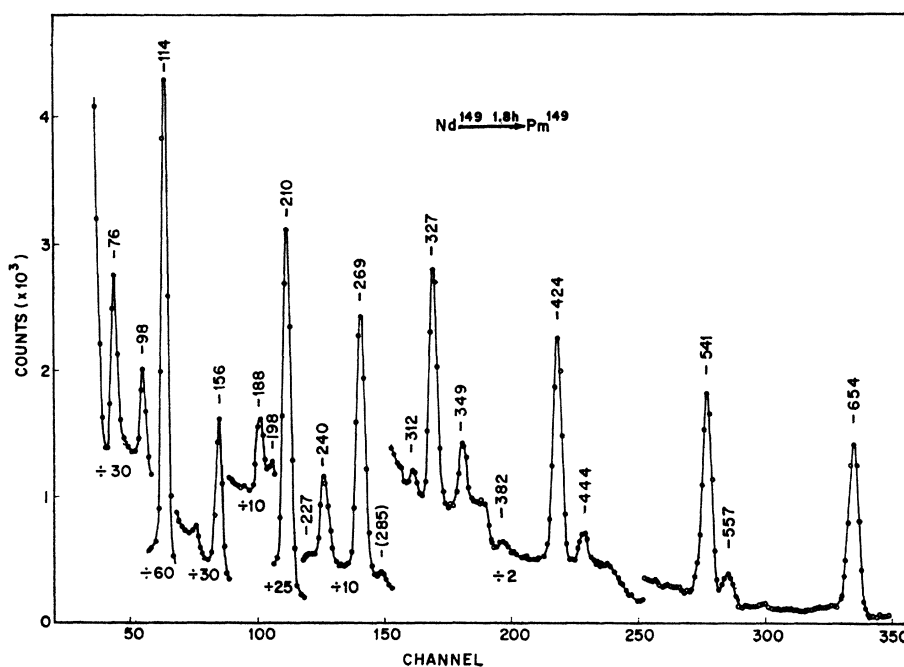


FIG. 3. Gamma-ray spectrum from the 1.8-h decay of Nd¹⁴⁹ as measured with a Ge(Li) solid-state detector. Parentheses indicate Pm¹⁴⁹ decay.

¹⁷ A. Schwarzschild, Nucl. Instr. Methods 21, 1 (1963).

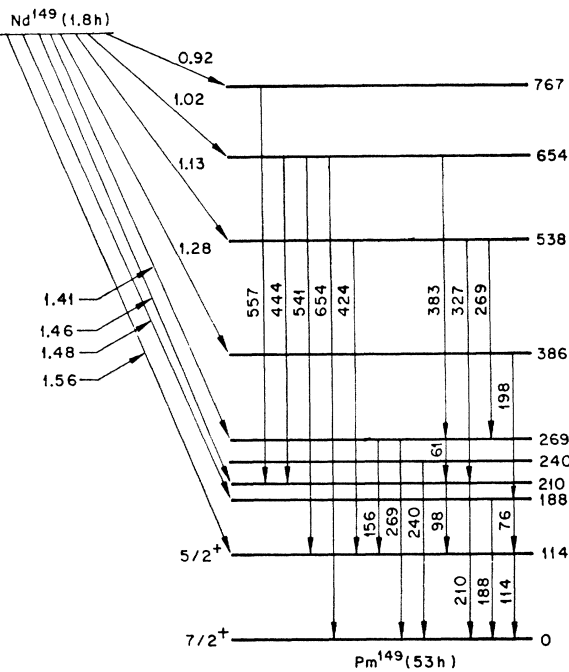


FIG. 4. Decay scheme of 1.8-h Nd^{149} suggested from Refs. 11-14. Only gamma rays from the present experiment which fit the level scheme are shown.

The lifetime measurement of the 114-keV level was obtained from the distribution of the delays between betas populating this level which have a 1.56-MeV endpoint and the decaying gamma rays. With the gamma acceptance channel set at the Compton edge of the 114-keV gamma ray, several lifetime measurements were made for various beta-energy channels. These channel settings were varied from beta energies of 1.2 to 1.5 MeV. At the lower energies a large detecting efficiency was achieved for betas populating the 114-keV level, however at the sacrifice of an increased

TABLE I. Gamma rays following the decay of Nd^{149} .

E_γ (keV)	Relative intensity
76	7
98	6
114	88
156	25
188	7
198	1
210	100
227	0.5
240	15
269	57
312	1
327	16
349	4
382	0.8
424	28
444	5
541	26
557	4
654	28

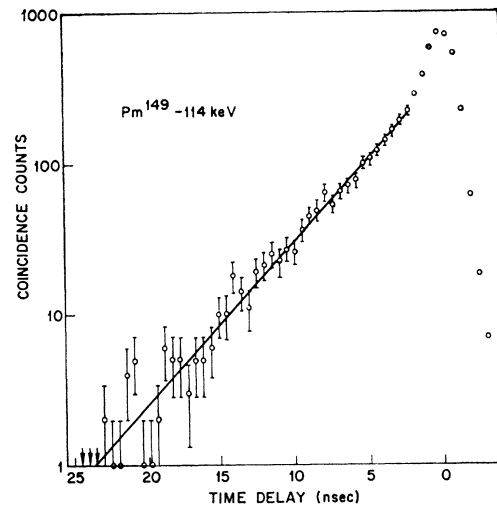


FIG. 5. Decay curve for the 114-keV level in Pm^{149} . The prompt peak is associated with the 210-keV level.

detection efficiency for other beta branches. For the higher energy channel settings, the desired beta branch was isolated but with only a low detection efficiency. The resulting measurements showed a slight increase in the observed lifetime as the beta channel was lowered as well as an increasing prompt peak. This suggested that one of the other detected beta branches populated a level with a measurable lifetime.

To investigate this possibility, a measurement was made with the beta channel fixed at 1.2 MeV but with the gamma channel set near the Compton edge of the 210-keV gamma ray. This measurement showed a strong prompt peak due to the 210-keV level and a significant lifetime for the 269-keV level. The beta branch to the 210-keV level is about 2.5 times as

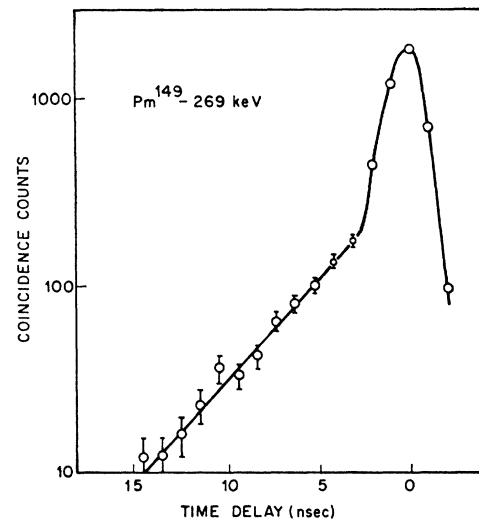


FIG. 6. Decay curve for the 269-keV level in Pm^{149} along with the large prompt contribution from the level at 210 keV.

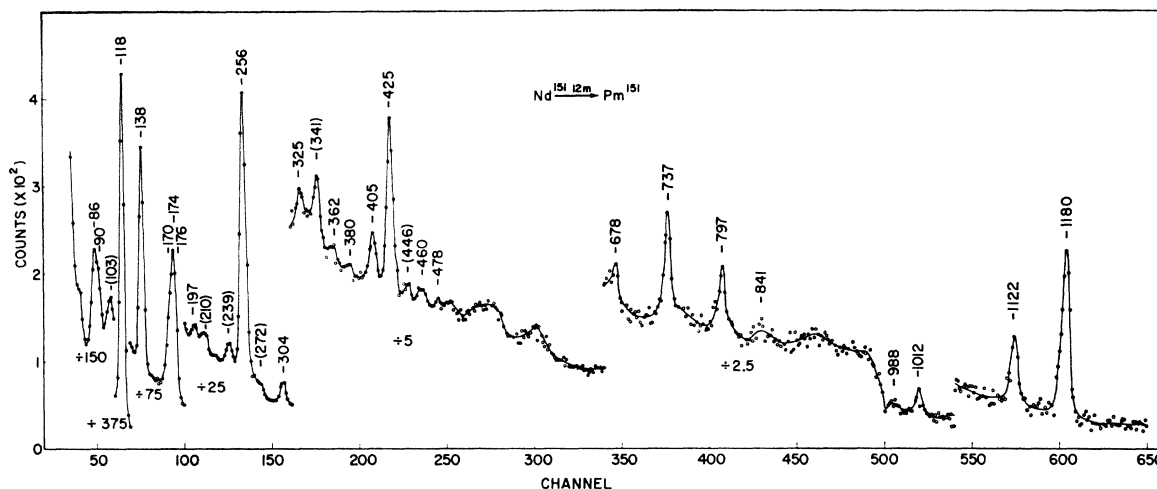


FIG. 7. Gamma-ray spectrum from the 12-min decay of Nd^{151} as measured with a Ge(Li) solid-state detector. Parentheses indicate Pm^{151} decay.

strong as those to the levels at 269 and 114 keV. Thus, to eliminate a mixture of the lifetime of the 269-keV level into the lifetime measurement of the 114-keV level, the beta channel must be set to discriminate against most of the 1.41-MeV beta branch. With this criterion satisfied and with the appropriate gamma channel the decay curve for the 114-keV state was obtained as shown in Fig. 5. From a least-squares fit to the logarithmic slope, the half-life of the $\frac{5}{2}^+$ 114-keV state in Pm^{149} was found to be $t_{1/2} = (2.62 \pm 0.10)$ nsec. The prompt peak seen in Fig. 5 is associated with the level at 210 keV.

The decay curve including the 210- and 269-keV levels as discussed above is shown in Fig. 6. From logarithmic slopes an upper limit of $t_{1/2} \leq 0.3$ nsec is placed on the half-life for the level at 210 keV and a half-life of $t_{1/2} = (2.7 \pm 0.2)$ nsec is obtained for the 269-keV level.

From the measured gamma-ray intensities and a knowledge of the beta branches, estimates of the influence of other lifetimes have been made for these measurements. The error limits listed include these estimates plus uncertainties resulting from statistics and the time calibration.

Pm^{151}

Lifetime measurements for low-energy states in Pm^{151} were obtained from the 12-min Nd^{151} beta decay. The gamma-ray spectrum from this activity as measured with the Ge(Li) solid-state detector is shown in Fig. 7. A list of the gamma-ray energies and intensities are given in Table II. Available data¹⁸ predict a level scheme for Pm^{151} as shown in Fig. 8. Gamma rays measured in the present experiment are shown where consistent with this level scheme. A portion of this scheme as indicated with dotted lines appears incon-

sistent with the present measurements. Also a number of weak gamma rays which have not been observed previously are not fit into the decay scheme.

Since betas have not been observed to populate the 118-keV level in Pm^{151} directly, a lifetime measurement was made between betas populating the 256-keV level and gamma rays from the 118-keV level; this technique takes advantage of the 138-keV-cascade gamma transition. With the appropriate channels a decay curve that indicated a lifetime was observed, as shown in Fig. 9. The distribution of time delays for this measurement is a function of both the 256- and 118-keV-level lifetimes. This decay curve would yield a good lifetime measurement for the 118-keV level provided the lifetime of the 256-keV was considerably shorter. This would not be unexpected because of the strong

TABLE II. Gamma rays following the decay of Nd^{151} .

E_γ (keV)	Relative intensity
86-90	12
118	100
138	16
170-174-176	26
197	1
256	28
304	3
325	1
362	0.2
380	0.6
405	3
425	12
460	2
478	0.5
678	2
737	12
797	8
841	0.5
988	2
1012	4
1122	6
1180	22

¹⁸L. C. Schmid and S. B. Burson, Phys. Rev. **115**, 178 (1959).

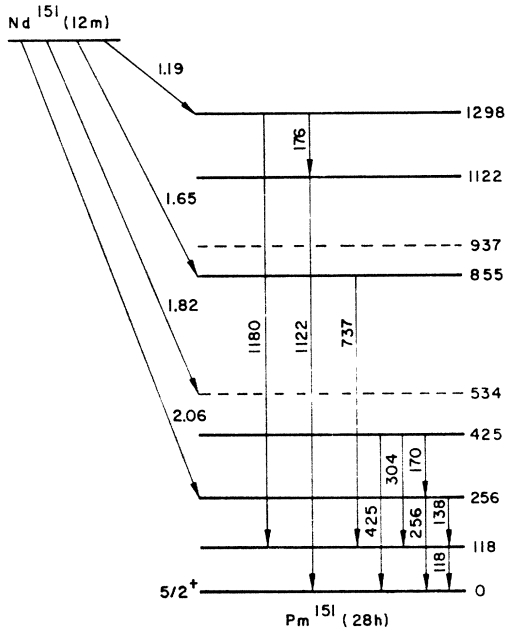


FIG. 8. Decay scheme of 12-min Nd^{151} as suggested in Ref. 18. Only gamma rays from the present experiment which fit the level scheme are shown.

energy dependence for the transition probabilities. Of course the converse is also true, where the lifetime of the 256-keV level could be obtained provided the lifetime for the 118-keV level is short.

This relation can be checked since the lifetime of the 256-keV level is easily isolated by raising the gamma channel to the Compton edge of the 256-keV gamma ray. The resulting decay curve for this measurement was identical to that in Fig. 9 which indicates that the observed decay curve is associated with the 256-keV level. From a least-squares fit to the slope, the half-life for the 256-keV level in Pm^{151} is $t_{1/2}$

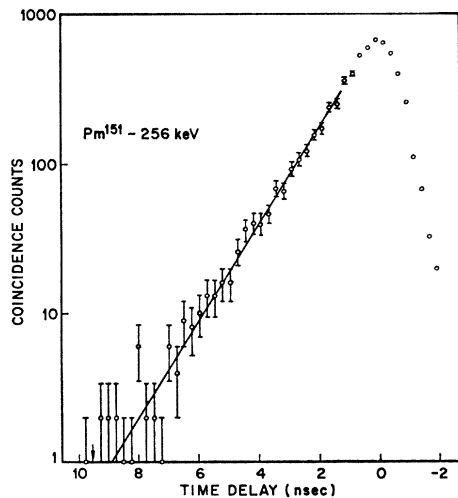


FIG. 9. Decay curve for the 256-keV level in Pm^{151} .

$= (0.91 \pm 0.03)$ nsec. With a gamma channel set at the Compton edge for 400-keV gammas only a weak prompt peak was observed.

To observe the short lifetime of the 118-keV level with greater sensitivity, a time-delay measurement was made between the intense 1180-keV gamma and the 118-keV gamma. This measurement which isolated the 118-keV level resulted in an upper limit of $t_{1/2} \leq 0.3$ nsec.

Sb¹²⁵

The lifetime of the $5/2^+$ first excited state in Sb^{125} at 326 keV was measured from the 9.7-min isomeric Sn^{125} activity. A 98% beta branch¹ with a 2.04-MeV end point populates this level as shown in Fig. 10. In this measurement the beta channel was set at about 1.5 MeV and the gamma channel at the Compton edge of the 326-keV gamma ray; these acceptance channels

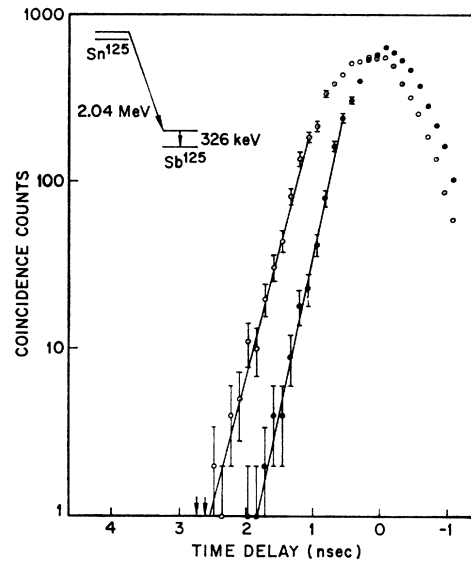


FIG. 10. Decay curve for the 326-keV level in Sb^{125} as shown with open circles. A prompt peak from Co^{60} is shown with filled circles. An abbreviated decay scheme of 9.7-min Sn^{125} is also displayed.

completely isolated this level. Because of the short 9.7-min activity, a rather high initial counting rate was required in order to obtain reasonable statistics; however, the rate was kept considerably below the limits of the electronics. The observed decay curve is shown in Fig. 10. A prompt peak taken with Co^{60} under the same channel conditions and with similar counting rates is shown by filled circles in Fig. 10. Since the two slopes are similar, only an upper limit of $t_{1/2} \leq 0.2$ nsec can be placed on the half-life of the 326-keV level of Sb^{125} .

Sm^{151} from the 28-h Pm^{151} Daughter Activity

The lifetimes of low-energy levels in Sm^{151} can be observed with the 28-h Pm^{151} daughter activity. The

TABLE III. Gamma rays following the decay of Pm^{151} .

E_γ (keV)	Relative intensity
76	0.3
103	42
140	2
162-167	51
177	13
209	16
233-238	24
275	40
325	5
341	100

gamma rays from this activity have been measured with the Ge(Li) solid-state detector; the related decay scheme¹ up to 350 keV in excitation is shown in Fig. 11. For interpretation of the lifetime results, the energies and intensities of these gamma rays are listed in Table III.

Lifetime measurements for levels in Sm^{151} were made with the beta channel at about 600 keV and gamma channels at Compton energies corresponding to gamma rays of 100, 170, and 250 keV. The decay curve obtained with the lowest-energy gamma channel is displayed in Fig. 12. The logarithmic slope corresponds to a half-life of 0.48 nsec. Results for the other two gamma-channel settings showed a prompt peak plus a small contribution of a lifetime with only poor statistics. With a knowledge of the decay scheme and the gamma-ray intensities the half-life $t_{1/2} = (0.48 \pm 0.03)$ nsec appears to be associated only with the 105-keV level in Sm^{151} although it is not completely separated from the lifetimes of higher energy levels such as the level at 167 keV. From the measurement with the 250-keV channel an upper limit of $t_{1/2} \leq 0.2$ nsec can be placed on the half-life of the 345-keV level in Sm^{151} .

III. EXPERIMENTAL RESULTS

From the Ge(Li) solid-state detector measurements, several gamma rays were observed in the decays of 1.8-h Nd^{149} and 12-min Nd^{151} which previously had been unobserved (see Figs. 3 and 7). For the Nd^{149} decay,¹⁹ new gamma rays were seen at 227, 240, 312,

TABLE IV. A summary of the lifetime results from the present experiment.

Nucleus	Energy (keV)	Half-life (nsec)
Pm^{149}	114	2.62 ± 0.10
Pm^{149}	210	≤ 0.3
Pm^{149}	269	2.7 ± 0.2
Pm^{151}	118	≤ 0.3
Pm^{151}	256	0.91 ± 0.03
Sb^{125}	326	≤ 0.2
Sm^{151}	105	0.48 ± 0.3
Sm^{151}	345	≤ 0.2

¹⁹ After completion of this paper, two studies of the Nd^{149} decay have been reported: L. D. McIsaac and R. G. Helmer,

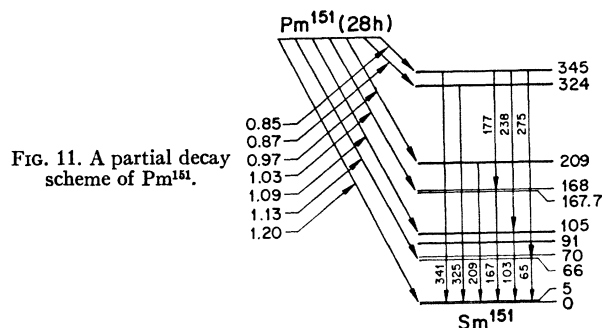


FIG. 11. A partial decay scheme of Pm^{151} .

349, and 557 keV and for the Nd^{151} decay at 197, 325, 362, 380, 460, 478, 797, 841, and 988 keV. Tables I and II include all of the observed gamma energies and intensities for the Nd^{149} and Nd^{151} decays, respectively. The additional structure in the gamma-ray spectra can be associated with the Compton effect.

A summary of the experimental lifetime results of the present paper is given in Table IV. An independent study of lifetimes for levels populated in the decay of Nd^{149} has been made by Currie *et al.*¹³ Their measurements were obtained from gamma-gamma coincidences using NaI crystals. This technique has the advantage of better isolation of individual gamma rays in a complex decay scheme; however, it has the disadvantage of a considerably larger time-resolution function. Their results for the levels in Pm^{149} are in agreement with those of the present experiment, except that a smaller upper limit for the lifetime of the 210-keV level is obtained in the present work.

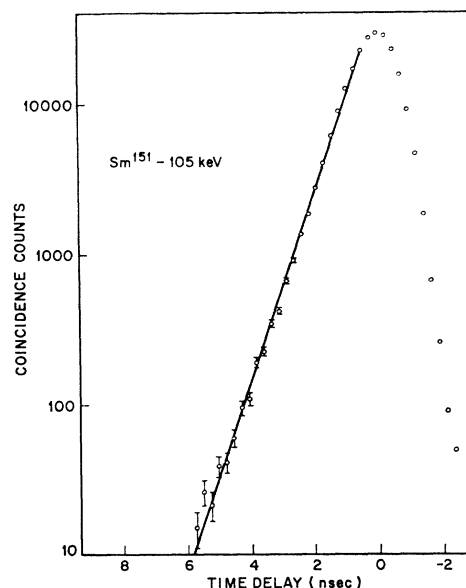


FIG. 12. Decay curve for the 105-keV level in Sm^{151} .

Bull. Am. Phys. Soc. 10, 442 (1965); E. B. Nieschmidt, V. R. Potnis, L. D. Ellsworth, and C. E. Mandeville, Bull. Am. Phys. Soc. 10, 442 (1965).

No previous results are available for comparison with the other lifetime measurements.

IV. DISCUSSION

To compare the degree of forbiddenness for the observed ($1g_{7/2} \leftrightarrow 2d_{5/2}$) $M1$ transitions, the usual hindrance factors $F = \tau_\gamma(M1)/\tau_{sp}$ (Moszk.) are calculated. These F factors are the ratio of the gamma lifetimes obtained experimentally to the theoretical single-particle (sp) estimates of Moszkowski.²⁰ The $M1$ gamma lifetime is given by $\tau_\gamma(M1) = 1.44(1 + \alpha_T) \times (1 + E2/M1)t_{1/2}$, where α_T is the total conversion coefficient. Theoretical conversion coefficients of Rose²¹ are used in this calculation. Although deviations from theoretical conversion coefficients exist where gamma matrix elements are hindered, experiments show that these deviations are not significant for this comparison. The term $E2/M1$ accounts for an admixture of $E2$ into the transition. From experimental information¹ on partial conversion coefficients, l -forbidden transitions of this type are expected to be predominantly $M1$. Thus, the $E2/M1$ ratio has been neglected.

The lifetimes, energies, and hindrance factors for the ($1g_{7/2} \leftrightarrow 2d_{5/2}$) l -forbidden transitions in four promethium and four antimony isotopes are shown in Table V.

TABLE V. Hindrance factors for l -forbidden $M1$ transitions.

Nucleus	Transition	E (keV)	$t_{1/2}$ (nsec)	F
$^{145}\text{Pm}_{84}$	$1g_{7/2} \rightarrow 2d_{5/2}$	61	2.7 ± 0.1^a	220
$^{147}\text{Pm}_{86}$	$2d_{5/2} \rightarrow 1g_{7/2}$	91	2.44 ± 0.08^b	330
$^{149}\text{Pm}_{88}$	$2d_{5/2} \rightarrow 1g_{7/2}$	114	2.62 ± 0.10^c	350
$^{151}\text{Pm}_{90}$	($\rightarrow 5/2$)	118	$\leq 0.3^e$	(≤ 40)
		256	0.91 ± 0.03^c	(650)
$^{119}\text{Sb}_{51}$	$1g_{7/2} \rightarrow 2d_{5/2}$	270	0.83 ± 0.02^d	150
$^{121}\text{Sb}_{70}$	$1g_{7/2} \rightarrow 2d_{5/2}$	37	3.5 ± 0.2^e	90
$^{123}\text{Sb}_{72}$	$2d_{5/2} \rightarrow 1g_{7/2}$	160	0.64 ± 0.05^f	130
$^{125}\text{Sb}_{74}$	$2d_{5/2} \rightarrow 1g_{7/2}$	326	$\leq 0.2^e$	≤ 300

^a R. L. Graham and R. E. Bell, Can. J. Phys. 31, 377 (1953).

^b E. Ye. Berlovich, G. M. Bukat, Yu. K. Gusev, V. V. Ilyin, V. V. Nikitin, and M. K. Nikitin, Phys. Letters 2, 344 (1962).

^c This work.

^d T. D. Nainan, Phys. Rev. 123, 1751 (1961).

^e Y. Y. Chu, O. C. Kistner, A. C. Li, S. Monaro, and M. L. Perlman, Phys. Rev. 133, B1361 (1964).

^f M. Schmorak, A. C. Li, and A. Schwarzschild, Phys. Rev. 130, 727 (1963).

²⁰ S. A. Moszkowski, in *Alpha-, Beta-, and Gamma-Ray Spectroscopy*, edited by K. Siegbahn (North-Holland Publishing Company, Amsterdam, 1965), p. 863.

²¹ M. E. Rose, *Internal Conversion Coefficients* (Interscience Publishers, New York, 1958).

Except for the uncertain transitions in Pm^{151} , the hindrance factors from the present experiment are consistent with those of the other isotopes. If adjustment is made for the statistical factor²² $(2J+1)$, these hindrances are even more uniform.

With the lifetime of the 118-keV level in Pm^{151} implying no hindrance for an $M1$ transition to the ground state, it is most probable that the Pm^{151} nucleus is sufficiently deformed such that the description of this transition in terms of ($1g_{7/2} \leftrightarrow 2d_{5/2}$) is no longer adequate. An alternative description is one based on the single-particle levels²³ for a deformed potential including the possibility of rotational bands. The observed magnetic moment 1.8 nm of the ground state is consistent with the $\frac{5}{2}^+$ [413] Nilsson level.¹ This level is available for Pm^{151} with a deformation $0.14 < \delta < 0.21$. It is then possible that the 118-keV level is a $\frac{3}{2}^+$ rotational level built on the ground state; the half-life of ≤ 0.3 nsec agrees with that expected for a transition within the band.²⁴ The lifetime measured for the 256-keV level suggests that it is another intrinsic state. Assuming a similar deformation, the next available level is the $\frac{3}{2}^+$ [411]. This appears to be a good choice since an $M1$ transition to the $\frac{5}{2}^+$ [413] violates certain selection rules.²³ An $M1$ hindrance has previously been observed for the transition between states in Eu^{153} which have the same description.²³ It is concluded that the levels in Pm^{151} are more appropriately described with a deformed nucleus rather than being considered as spherical-potential states such as in the ($1g_{7/2} \leftrightarrow 2d_{5/2}$) transitions.

The collective influence⁸ previously observed on the l -forbidden transitions of $\text{Eu}^{147,149,151}$ does not appear as strong for the $\text{Pm}^{145,147,149}$ group, since the hindrance factors are all similar. Although, if the 118-keV transition in Pm^{151} were predominantly of the ($1g_{7/2} \leftrightarrow 2d_{5/2}$) type, this transition could be viewed as a collective enhancement.

Theoretical matrix elements for these hindered transitions calculated for configuration mixing by Arima *et al.*² are within a factor of about 2 of the experimental values.

²² D. H. Wilkinson, in *Nuclear Spectroscopy, Part B*, edited by F. Ajzenberg-Selove (Academic Press Inc., New York, 1960), p. 582.

²³ B. R. Mottelson and S. G. Nilsson, Kgl. Danske Videnskab. Selskab, Mat. Fys. Skrifter 1, No. 8 (1959).

²⁴ A. Bohr and B. R. Mottelson, Kgl. Danske Videnskab. Selskab, Mat. Fys. Medd. 27, No. 16 (1957).